



*Supplement of*

**Measurement report: Vertical distribution of atmospheric particulate matter within the urban boundary layer in southern China – size-segregated chemical composition and secondary formation through cloud processing and heterogeneous reactions**

**Shengzhen Zhou et al.**

*Correspondence to:* Shengzhen Zhou (zhoushz3@mail.sysu.edu.cn) and Xuemei Wang (eeswxm@mail.sysu.edu.cn)

The copyright of individual parts of the supplement might differ from the CC BY 4.0 License.

## 1. PMF model

A positive matrix factorization (PMF) model was used to resolve mass size distribution modes. PMF is a commonly used multivariate factor analysis technique that is capable of decomposing the aerosol chemical species data matrix into two matrices, factor profiles and factor contributions:

5

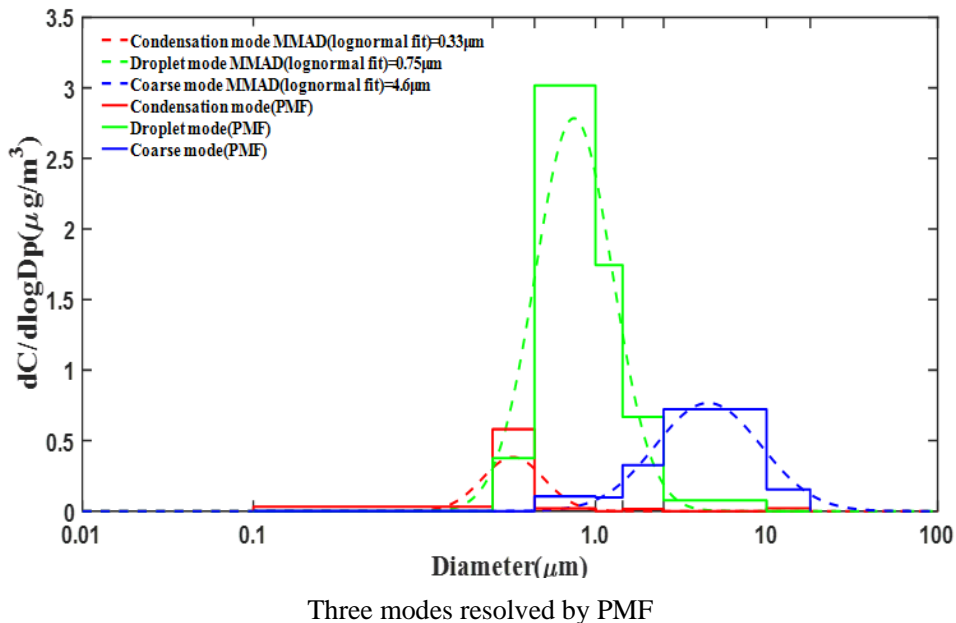
$$x_{ij} = \sum_{k=1}^p g_{ik} f_{kj} + e_{ij} \quad (1)$$

and

$$Q = \sum_{i=1}^n \sum_{j=1}^m \left[ \frac{x_{ij} - \sum_{k=1}^p g_{ik} f_{kj}}{u_{ij}} \right]^2 \quad (2)$$

where the element  $x_{ij}$  is the concentration value of the  $i$ th sample at the  $j$ th size interval or species;  $g_{ik}$  is the amount of mass contributed from the  $k$ th source associated with the  $i$ th sample and  $f_{kj}$  is the size distribution or species profile associated with the  $k$ th source;  $e_{ij}$  is the residual for each sample or species. The aim of the PMF solution is to minimize the object function  $Q$  (Eq. (2)) via a conjugate gradient algorithm, based upon estimated data uncertainties (or adjusted data uncertainties)  $u_{ij}$  (Brown et al., 2015). In this work, the EPA PMF 5.0 software package was used to perform the calculation (Norris et al., 2014). The uncertainties for the observed data were prepared based on the recommended method in the EPA PMF 5.0 manual. PMF was proved to be an efficient method to resolve overlapped modes of particle size distribution in early works (Guo et al, 2010; Liu et al, 2015). Totally 540 sets (30 samples  $\times$  6 species  $\times$  3 levels) of mass size distribution data were generated at the 3 heights (the ground level, 118 m, and 488 m) of Canton Tower. Six species include  $K^+$ ,  $NH_4^+$ ,  $SO_4^{2-}$ ,  $Cl^-$ ,  $Na^+$ , and  $NO_3^-$  at each height respectively. PMF analysis was executed on these 540 sets of data. At last, 3 factors implying 3 modes marked by their peaks were chosen to obtain the most reasonable solution.

The following figure shows the 3 PMF resolved size distribution modes fitted by lognormal function through Matlab software to determine mass medium aerodynamic diameters (MMAD) and eventually explaining 94% of total measured aerosol mass. The MMAD in this work was 0.33, 0.75, 4.6  $\mu m$  corresponding condensation mode, droplet mode and coarse mode respectively, which presented a remarkable similarity to former urban aerosol research in Hong Kong (Gao et al. 2016). PMF resolved average particle concentrations for each mode at ground level, 118 m, and 488 m during autumn and winter campaigns were showed in **Table S1**.



## 5 References:

- Brown, S. G., Eberly, S., Paatero, P., and Norris, G. A.: Methods for estimating uncertainty in PMF solutions: Examples with ambient air and water quality data and guidance on reporting PMF results, *Sci. Total Environ.*, 518, 626-635, <http://dx.doi.org/10.1016/j.scitotenv.2015.01.022>, 2015.
- Gao, Y., Lee, S. C., Huang, Y., Chow, J. C., and Watson, J. G.: Chemical Characterization and Source Apportionment of Size-Resolved Particles in Hong Kong Sub-Urban Area, *Atmospheric Research*, 170, 112-22, <http://dx.doi.org/10.1016/j.atmosres.2015.11.015>, 2016.
- Guo, S., Hu, M., Wang, Z., Slanina, J., and Zhao, Y.: Size-resolved aerosol water-soluble ionic compositions in the summer of Beijing: implication of regional secondary formation. *Atmos. Chem. Phys.* 10, 947-959, <https://doi.org/10.5194/acp-10-947-2010>, 2010.
- Liu, Z., Xie, Y.Z., Hu, B., Wen, T. X., Xin, J.Y., Li, X. R., and Wang, Y. S.: Size-resolved aerosol water-soluble ions during the summer and winter seasons in Beijing: Formation mechanisms of secondary inorganic, *Chemosphere*, 183, 119-131, <http://dx.doi.org/10.1016/j.chemosphere.2017.05.095>, 2017.
- Norris, G., Duvall, R., Brown, S., and Bai, S.: EPA Positive Matrix Factorization (PMF) 5.0 fundamentals and User Guide Prepared for the US Environmental Protection Agency Office of Research and Development, Washington, DC., 2014.

## 2. Analytical and sampling uncertainty analysis

The sampling uncertainty may originate from (a) the sampling flow rate, and (b) possibly from the impacts of temperature and pressure due to the sampling heights.

Three impactors (or samplers) were calibrated using mass flow meter (TSI, model 4040) in the laboratory before they were used during the study. The flow rates of the impactors were measured at the beginning of the sampling. At the end of the sampling period, the flow rates were recorded again. If the flow rate of each impactor at the beginning and end of the sampling period differed by more than 10%, the sample was marked as suspect and the data was discarded. The average flow rates at the beginning and end of the sampling time was used as the sampling flow rate. In addition, a magnehelic pressure gauge was used to monitor the inlet flow rate through the impactor. The pressure drop was also recorded at the beginning and end of sampling.

We actually did not adjust to standard conditions given the vertical height is less than 500 m and the impacts are small. To prove this, we calculated the impacts of pressure and temperature on the flow rate, and found that these impacts were less than 5%. Blows are our simple calculations based on the measurements of relevant parameters on the Canton tower on Oct. 23, 2015:

The daily average temperatures were 28.0 °C and 24.1 °C at the ground level and 488 m, respectively. And the daily average atmospheric pressures were 101.15 kPa and 95.72 kPa at these two levels. The flow rate at the ground level is 100 L/min. We calculated the flow rate when the temperature was 24.1 °C and the pressure was 95.72 kPa, i.e. at 488 m, assuming a flow rate of 100 L/m<sup>3</sup> at the ground level (temperature = 301.15 K and pressure = 101.15 kPa).

Assume the ambient air is an ideal gas. At the ground level,  $P_1 = 101.15 \text{ kPa}$ ,  $V_1 = 100 \text{ L/min}$ ,  $T_1 = 273.15 + 28 = 301.15 \text{ K}$ . At 488 m,  $P_2 = 95.72 \text{ kPa}$ ,  $V_2 = ?$ ,  $T_2 = 273.15 + 24.1 = 297.25 \text{ K}$ .  $R$  is the ideal gas constant.  $n$  is the moles of air.

$$\text{We obtain: } P_1 V_1 = nRT_1 \quad (1)$$

$$P_2 V_2 = nRT_2 \quad (2)$$

(1)/(2) we get:

$$V_2 = \frac{P_1 V_1 T_2}{P_2 T_1} = \frac{101.15 \times 100 \times 297.25}{95.72 \times 301.15} = 104.3 \text{ L/min}$$

We conclude that the impacts of pressure and temperature on the flow rate are less than 5%.

### 3. Estimation of secondary organic carbon concentration

It is difficult to separate primary organic carbon (POC) from secondary organic carbon (SOC). Currently, no simple, direct analytical technique is available for the separation. Here we applied an indirect method (the minimum OC/EC ratio method) to estimate the secondary organic carbon ( $OC_{sec}$ ) formation with the following equation (Cao et al., 2004; Castro et al., 1999; Zhou et al., 2014):

$$OC_{sec} = OC_{tot} - EC \times (OC/EC)_{min}$$

where  $OC_{sec}$  is secondary organic carbon,  $OC_{tot}$  is total organic carbon, EC is elemental carbon, and  $(OC/EC)_{min}$  is the minimum OC/EC ratio. The minimum ratio of OC/EC may be affected by many factors such as meteorological conditions, the variation of the emission source, and the transport of aged aerosols. Thus, SOC concentration derived by the EC tracer method could be underestimated in this study. In order to reduce this uncertainty, the  $(OC/EC)_{min}$  is defined as the minimum OC/EC ratio of each size interval at each height in autumn and winter respectively.

### References:

- 15 Cao, J. J., Lee, S. C., Ho, K. F., Zou, S. C., Fung, K., Li, Y., Watson, J. G., and Chow, J. C.: Spatial and seasonal variations of 25 atmospheric organic carbon and elemental carbon in Pearl River Delta Region, China, *Atmos. Environ.*, 38, 4447-4456, <https://doi.org/10.1016/j.atmosenv.2004.05.016>, 2004.
- Castro, L.M., Pio, C.A., Harrison, R.M., Smith, D.J.T., 1999. Carbonaceous aerosol in urban and rural European atmospheres: estimation of secondary organic carbon concentrations. *Atmos. Environ.* 33, 2771e2781.  
20 [http://dx.doi.org/10.1016/s1352-2310\(98\)00331-8](http://dx.doi.org/10.1016/s1352-2310(98)00331-8).
- Zhou, S. Z., Wang, T., Wang, Z., Li, W. J., Xu, Z., Wang, X. F., Yuan, C., Poon, C. N., Louie, Peter K.K., Luk, Connie W.Y., and Wang, W. X: Photochemical evolution of organic aerosols observed in urban plumes from Hong Kong and the Pearl River Delta of China, *Atmos. Environ.*, 88, 219–229, <http://dx.doi.org/10.1016/j.atmosenv.2014.01.032>, 2014.

**Table S1** Vertical distributions of major PM<sub>2.5</sub> components in autumn and winter field studies.

Date	SO <sub>4</sub>	NO <sub>3</sub>	NH <sub>4</sub>	OC	EC	PM <sub>2.5</sub>
	category	category	category	category	category	µg/m <sup>3</sup>
2015/10/21	I	I	I	II	I	48.4
2015/10/23	II	II	III	II	I	59.1
2015/10/25	II	II	II	II	I	45.7
2015/10/26	II	II	II	II	I	41.5
2015/10/27	III	II	II	II	I	53.9
2015/10/29	II	II	II	II	I	40.6
2015/10/31	III	III	III	I	II	20.2
2015/11/02	I	I	III	I	I	34.6
2015/11/04	II	II	II	I	I	62.0
2015/11/06	III	III	III	I	I	43.3
2015/11/08	II	II	II	II	II	39.2
2015/11/10	III	III	III	I	II	40.0
2015/11/12	I	III	III	I	II	47.6
2015/11/14	II	II	II	I	II	36.8
2015/11/16	II	II	II	I	I	29.5
2015/11/18	III	III	III	I	I	76.0
2015/11/20	III	III	III	I	I	64.6
2015/11/22	III	I	III	I	II	34.2

Date	SO <sub>4</sub>	NO <sub>3</sub>	NH <sub>4</sub>	OC	EC	PM <sub>2.5</sub>
	category	category	category	category	category	µg/m <sup>3</sup>
2015/12/31	III	III	III	I	II	61.3
2016/01/02	II	II	II	II	I	104.8
2016/01/03	I	II	II	II	I	87.2
2016/01/04	II	II	II	I	II	54.4
2016/01/07	I	I	I	I	I	42.6
2016/01/09	II	II	III	I	I	65.8
2016/01/12	I	III	III	I	I	31.7
2016/01/13	I	I	I	I	I	37.3
2016/01/17	I	I	I	I	I	20.6
2016/01/18	I	II	I	II	I	35.2
2016/01/20	I	I	I	II	II	33.9
2016/01/25	I	I	I	I	I	24.5

Category I: concentrations peaking at the ground level.

Category II: concentrations peaking at 118 m.

Category III: concentrations peaking at 488 m.

PM<sub>2.5</sub> concentrations were recorded at the ground level.

**Table S2** The percentages of the three types in autumn and winter campaigns

Autumn	SO4	NO3	NH4	OC	EC
Category I	17%	17%	6%	72%	67%
Category II	44%	50%	44%	28%	33%
Category III	39%	33%	50%	0%	0%

Winter	SO <sub>4</sub> <sup>2-</sup>	NO <sub>3</sub> <sup>-</sup>	NH <sub>4</sub> <sup>+</sup>	OC	EC
Category I	67%	42%	50%	58%	58%
Category II	25%	42%	25%	42%	42%
Category III	8%	17%	25%	0%	0%

5

10

15

20

25

**Table S3.** PMF resolved average particle concentrations for each mode at ground level, 118 m and 488 m during autumn and winter campaigns.

		Condensation mode ( $\mu\text{g}/\text{m}^3$ )		Droplet mode ( $\mu\text{g}/\text{m}^3$ )		Coarse mode ( $\mu\text{g}/\text{m}^3$ )	
		autumn	winter	autumn	winter	autumn	winter
	ground	0.05 $\pm$ 0.03	0.11 $\pm$ 0.07	0.21 $\pm$ 0.09	0.39 $\pm$ 0.35	0.05 $\pm$ 0.02	0.04 $\pm$ 0.03
<b>K<sup>+</sup></b>	118m	0.05 $\pm$ 0.03	0.12 $\pm$ 0.09	0.18 $\pm$ 0.08	0.37 $\pm$ 0.31	0.06 $\pm$ 0.02	0.04 $\pm$ 0.03
	488m	0.03 $\pm$ 0.01	0.04 $\pm$ 0.03	0.15 $\pm$ 0.07	0.2 $\pm$ 0.17	0.03 $\pm$ 0.01	0.03 $\pm$ 0.02
	ground	0.2 $\pm$ 0.15	0.46 $\pm$ 0.22	1.21 $\pm$ 0.78	2.64 $\pm$ 2.34	0.05 $\pm$ 0.07	0.14 $\pm$ 0.22
<b>NH<sub>4</sub><sup>+</sup></b>	118m	0.24 $\pm$ 0.21	0.48 $\pm$ 0.27	1.4 $\pm$ 0.9	2.23 $\pm$ 2.52	0.12 $\pm$ 0.12	0.15 $\pm$ 0.22
	488m	0.07 $\pm$ 0.08	0.38 $\pm$ 0.13	1.63 $\pm$ 0.78	1.85 $\pm$ 2.01	0.12 $\pm$ 0.09	0.19 $\pm$ 0.23
	ground	0.53 $\pm$ 0.43	0.95 $\pm$ 0.43	4.23 $\pm$ 2.26	6.45 $\pm$ 4.06	0.57 $\pm$ 0.25	0.82 $\pm$ 0.83
<b>SO<sub>4</sub><sup>2-</sup></b>	118m	0.59 $\pm$ 0.49	0.99 $\pm$ 0.49	4.45 $\pm$ 2.32	6.2 $\pm$ 3.9	0.63 $\pm$ 0.28	0.68 $\pm$ 0.83
	488m	0.25 $\pm$ 0.17	0.71 $\pm$ 0.25	4.52 $\pm$ 2.17	5.26 $\pm$ 4.64	0.43 $\pm$ 0.24	0.57 $\pm$ 0.53
	ground	0.03 $\pm$ 0.1	0.03 $\pm$ 0.03	0.12 $\pm$ 0.21	0.94 $\pm$ 1.6	0.52 $\pm$ 0.47	0.35 $\pm$ 0.39
<b>Cl<sup>-</sup></b>	118m	0.03 $\pm$ 0.11	0.05 $\pm$ 0.06	0.06 $\pm$ 0.1	1.1 $\pm$ 1.82	0.72 $\pm$ 0.68	0.31 $\pm$ 0.35
	488m	0 $\pm$ 0.01	0.01 $\pm$ 0.02	0.08 $\pm$ 0.08	0.22 $\pm$ 0.31	0.31 $\pm$ 0.22	0.2 $\pm$ 0.35
	ground	0.03 $\pm$ 0.01	0.03 $\pm$ 0.04	0.06 $\pm$ 0.04	0.12 $\pm$ 0.11	0.52 $\pm$ 0.44	0.12 $\pm$ 0.18
<b>Na<sup>+</sup></b>	118m	0.04 $\pm$ 0.02	0.04 $\pm$ 0.04	0.01 $\pm$ 0.01	0.12 $\pm$ 0.11	0.61 $\pm$ 0.53	0.11 $\pm$ 0.15
	488m	0.01 $\pm$ 0.01	0.01 $\pm$ 0.02	0.04 $\pm$ 0.05	0.07 $\pm$ 0.05	0.45 $\pm$ 0.33	0.11 $\pm$ 0.23
	ground	0.09 $\pm$ 0.08	0.43 $\pm$ 0.33	0.46 $\pm$ 0.44	5.93 $\pm$ 7.9	2.39 $\pm$ 1.39	1.46 $\pm$ 1.43
<b>NO<sub>3</sub><sup>-</sup></b>	118m	0.15 $\pm$ 0.12	0.45 $\pm$ 0.31	0.88 $\pm$ 0.87	6.53 $\pm$ 8.34	2.99 $\pm$ 1.87	1.34 $\pm$ 1.69
	488m	0.07 $\pm$ 0.09	0.16 $\pm$ 0.17	0.74 $\pm$ 0.85	3.28 $\pm$ 3.53	2.25 $\pm$ 1.34	1.4 $\pm$ 1.41

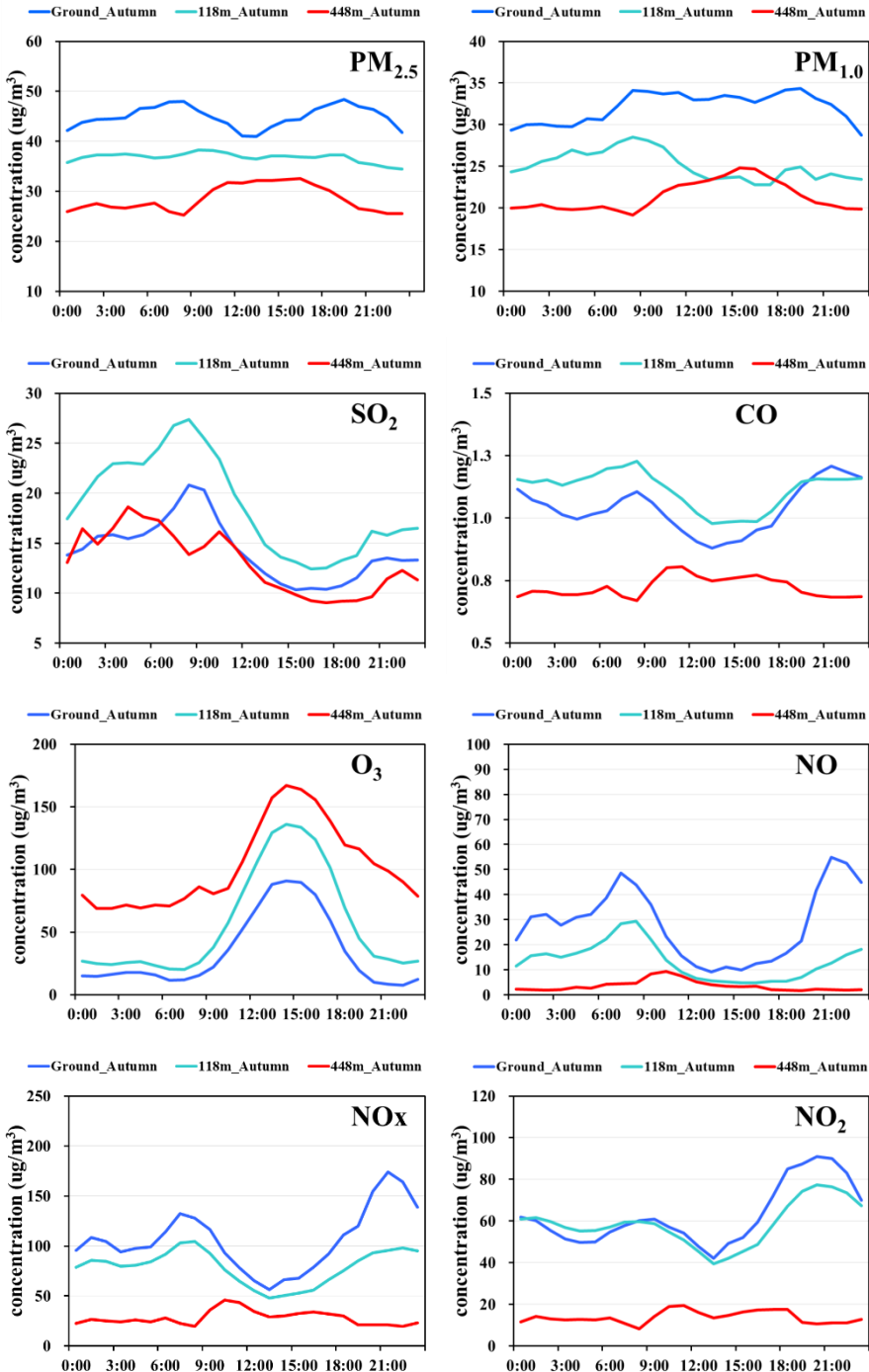


**Figure S1.** Diurnal variations of concentrations of pollutants at different altitudes on the Canton Tower during the autumn field study.

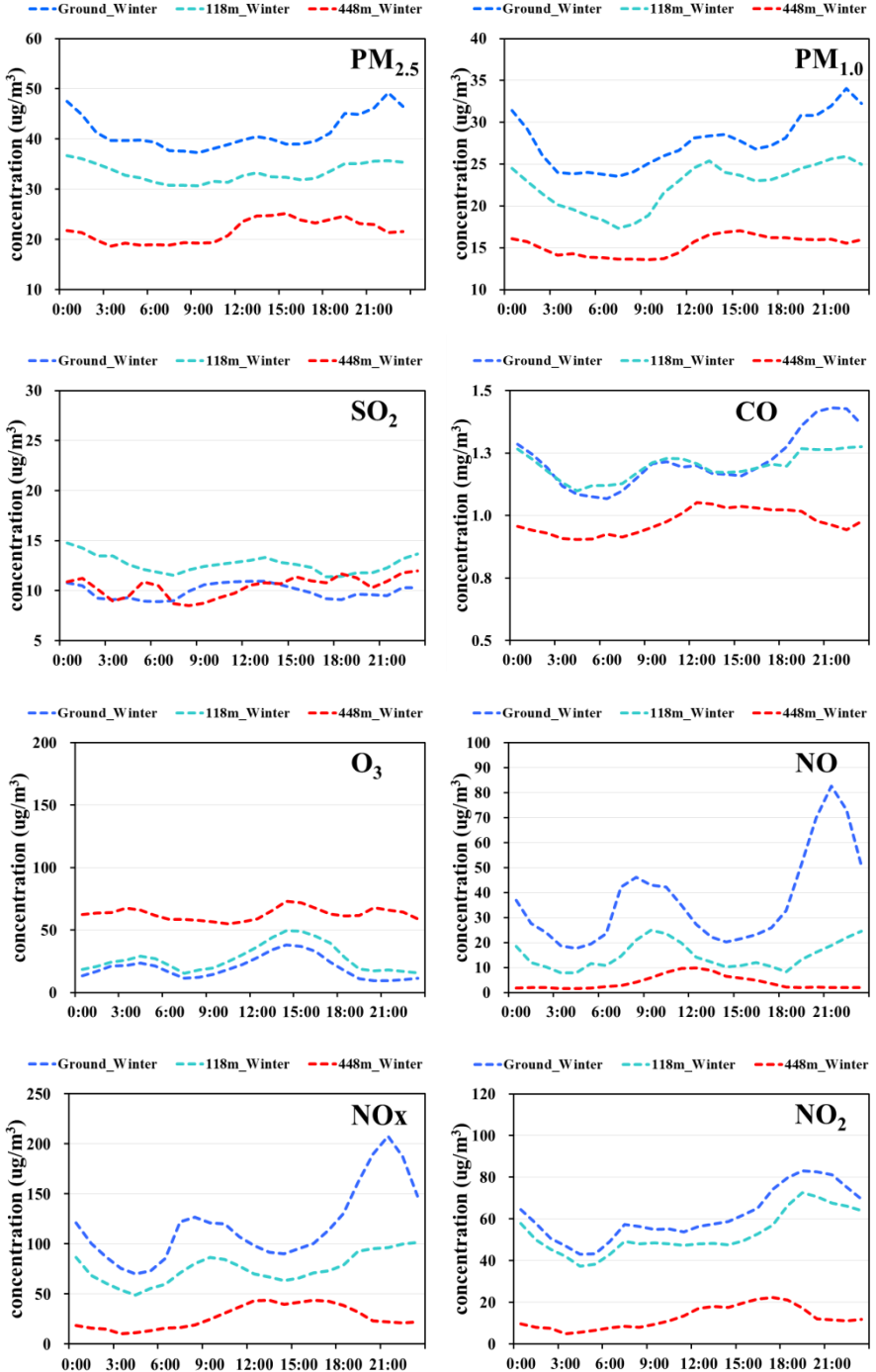


**Figure S2.** Diurnal variations of concentrations of pollutants at different altitudes on the Canton Tower during the winter field study.

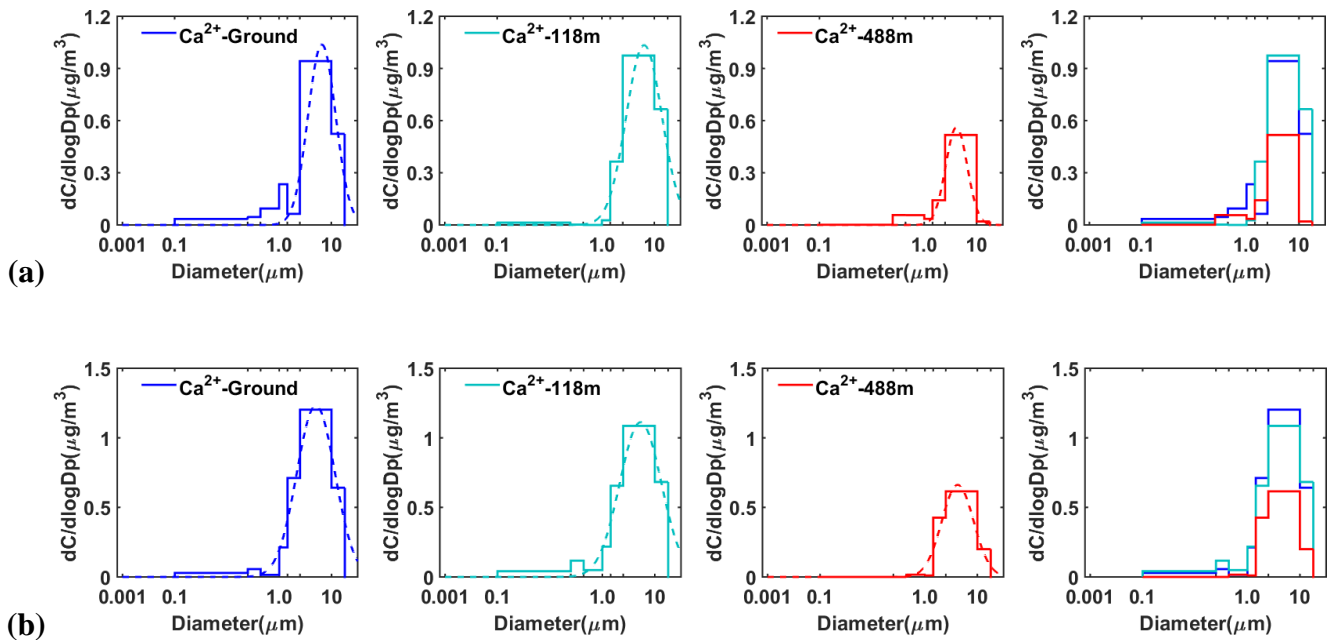


**Figure S3.** Mass concentration size distributions of  $\text{Ca}^{2+}$  measured at ground, 118 m and 488 m in winter: (a) autumn; (b) winter.

10

15

20

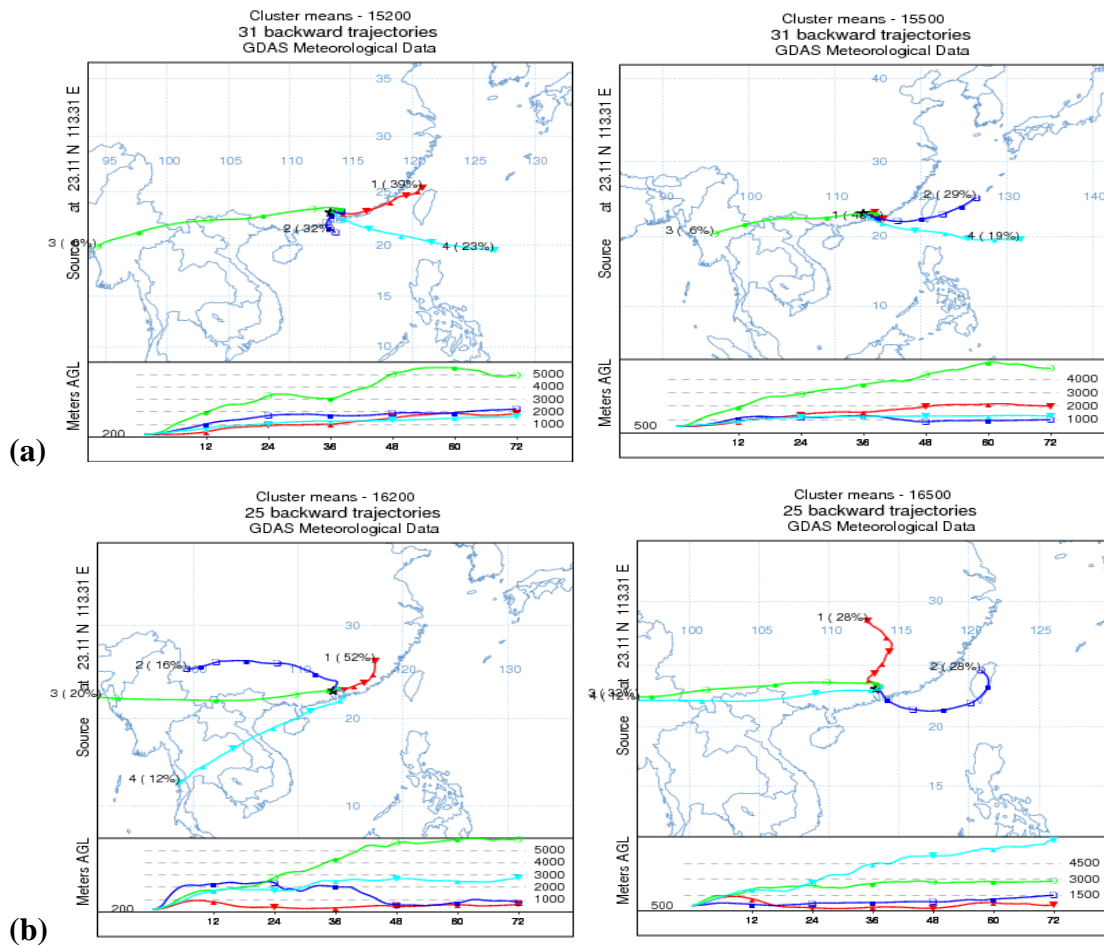


**Figure S4.** Cluster analysis of the airflow in 200 m and 500 m in (a) autumn and (b) winter periods.

5

10

15

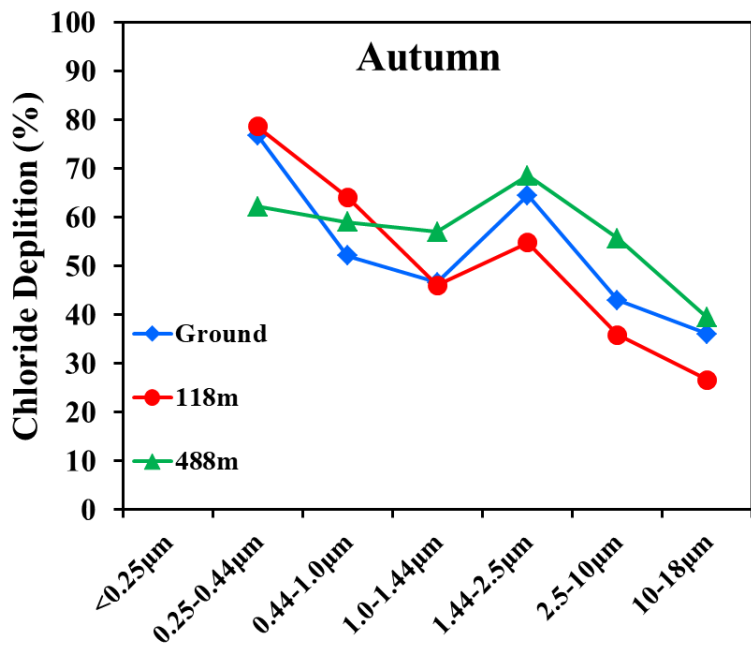


**Figure S5.** The percentage of chloride depletion at the three altitudes in autumn.

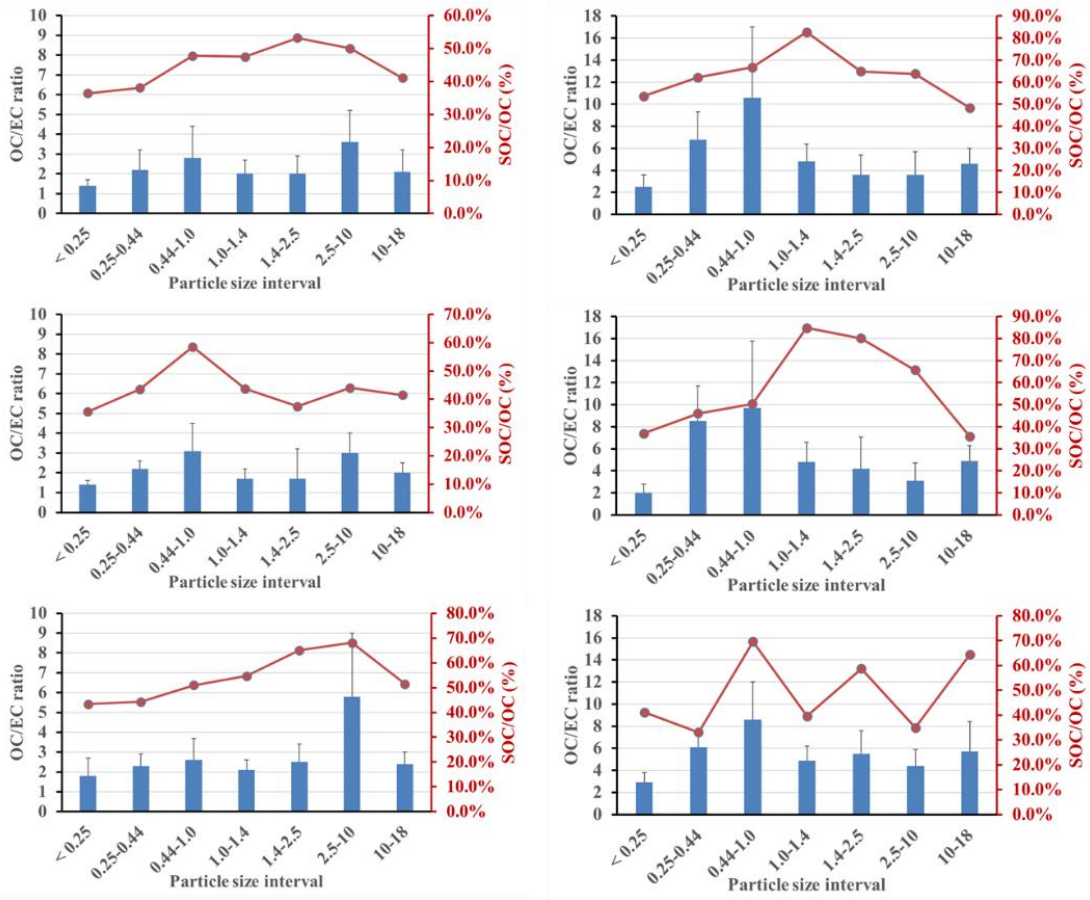


**Figure S6.** Average OC/EC ratios and percentages of SOC in OC at different sizes during autumn and winter.

5

10

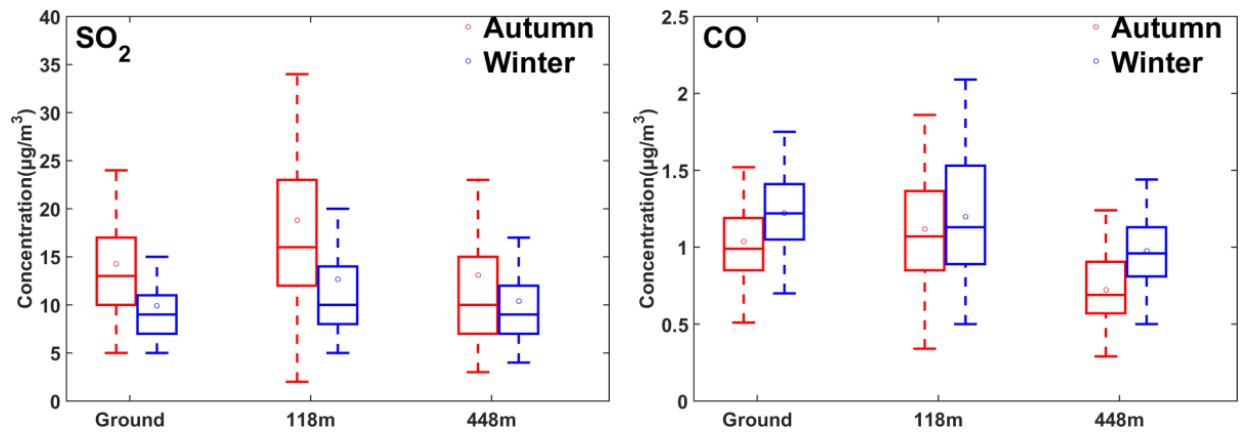


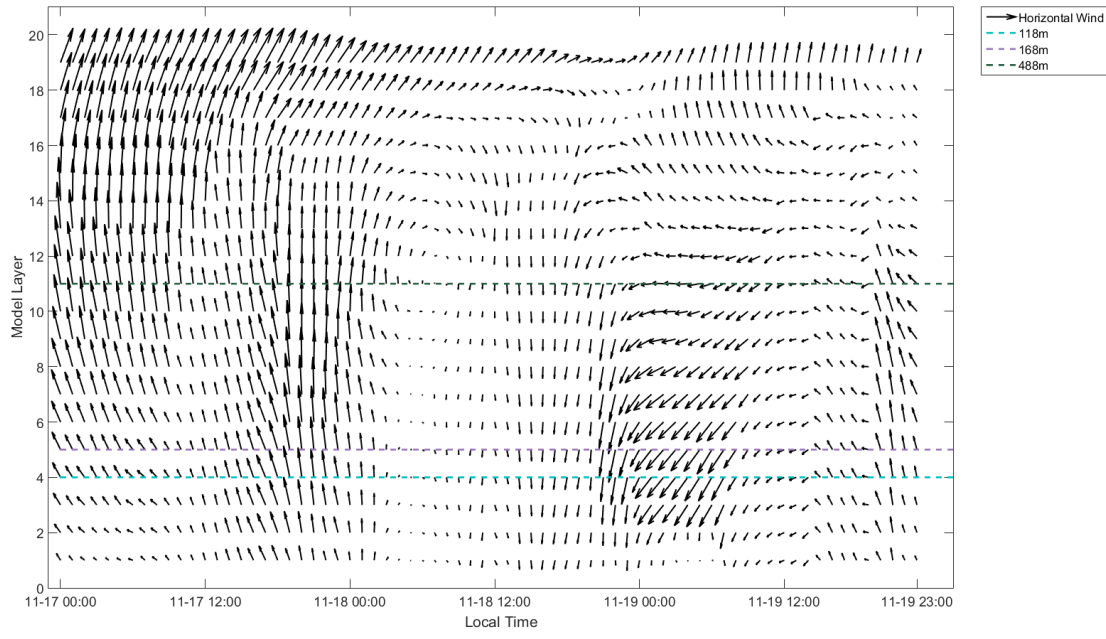
**Figure S7.** Concentration statistics of SO<sub>2</sub> and CO at different heights during the autumn and winter campaigns.

5

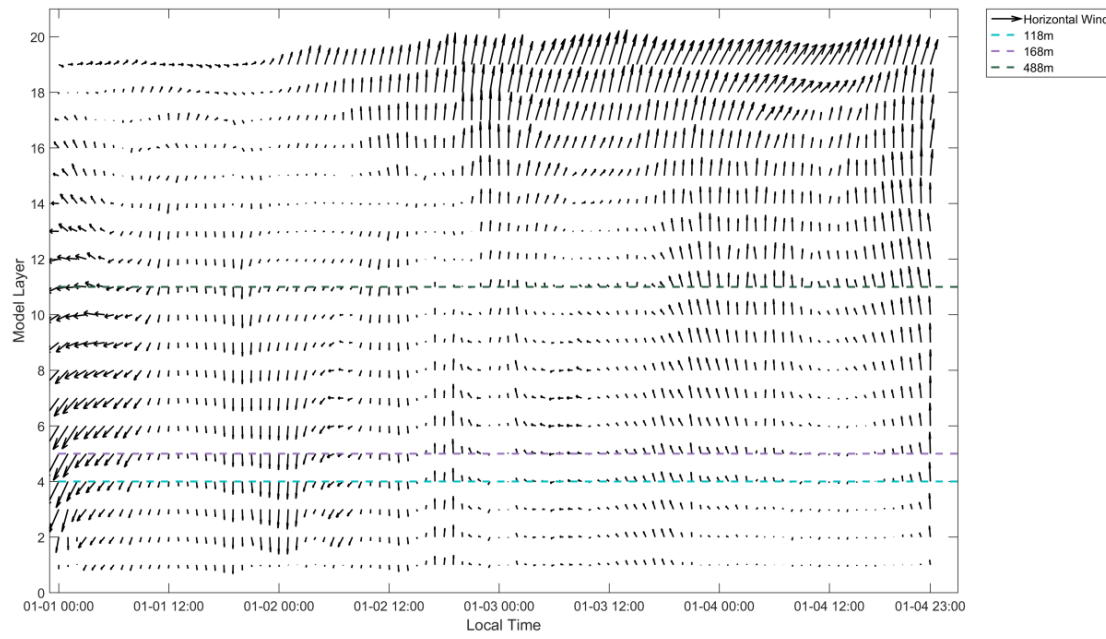
10

15

20



(a)



(b)

**Figure S8.** Modeled horizontal wind at different altitudes during (a) E1 episode in autumn; (b) E2 episode in winter.

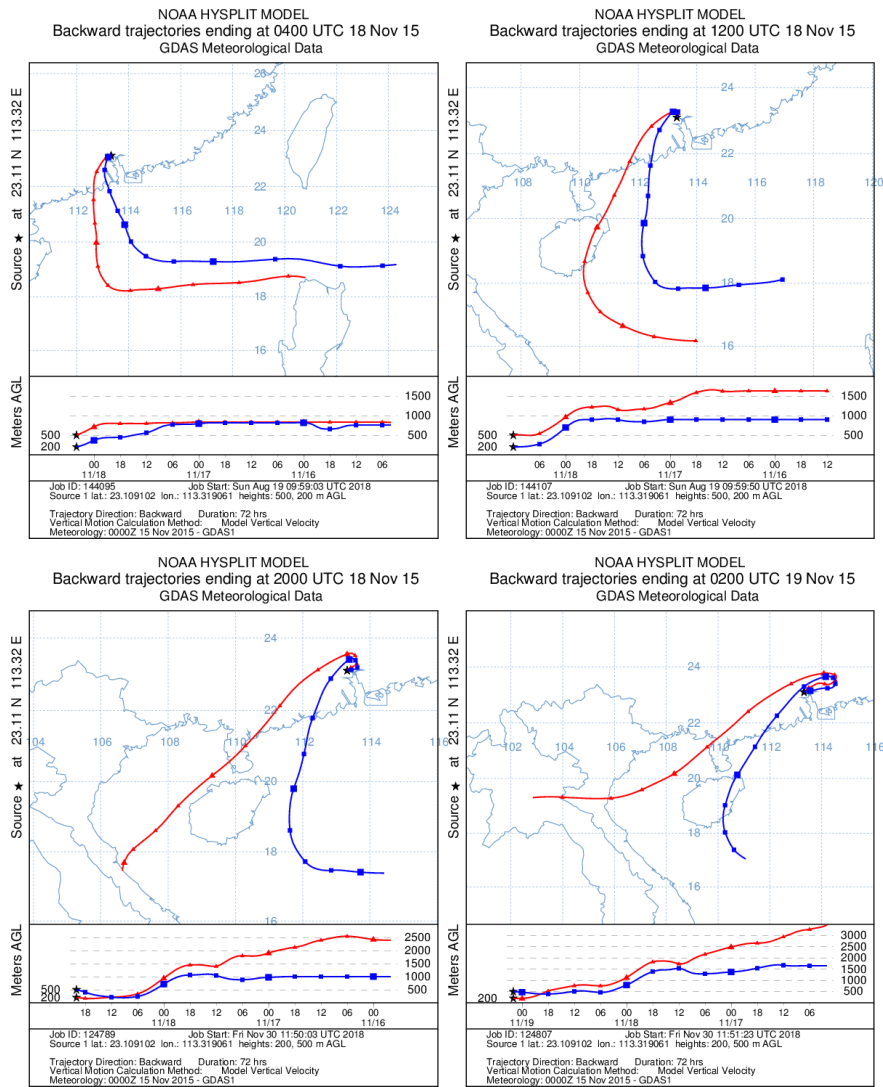
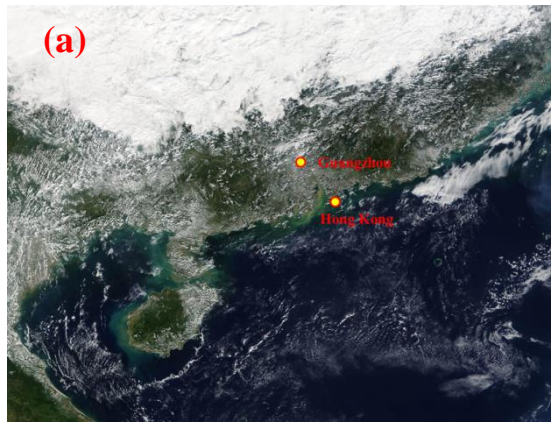
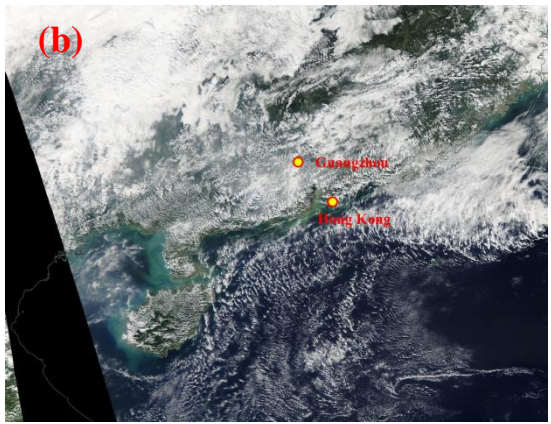


**Figure S9.** 72 h air mass back-trajectories analysis ending at the Canton Tower with height of 200 m and 500 m during

5 E1 episode in autumn.



(a) November 18, 2015



(b) November 19, 2015

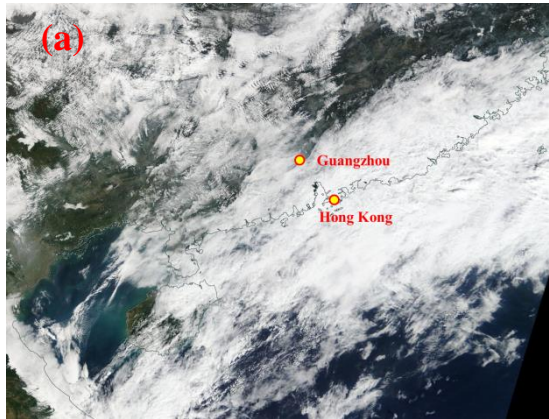
**Figure S10.** MODIS images show the cloud covers over the PRD region during the autumn pollution episode

5 (<https://earthdata.nasa.gov/earth-observation-data/near-real-time/rapid-response>).

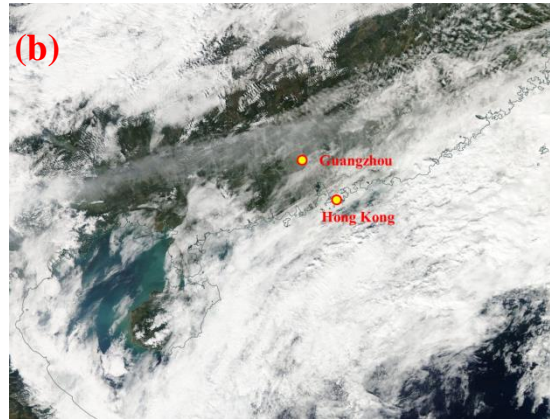
10

15

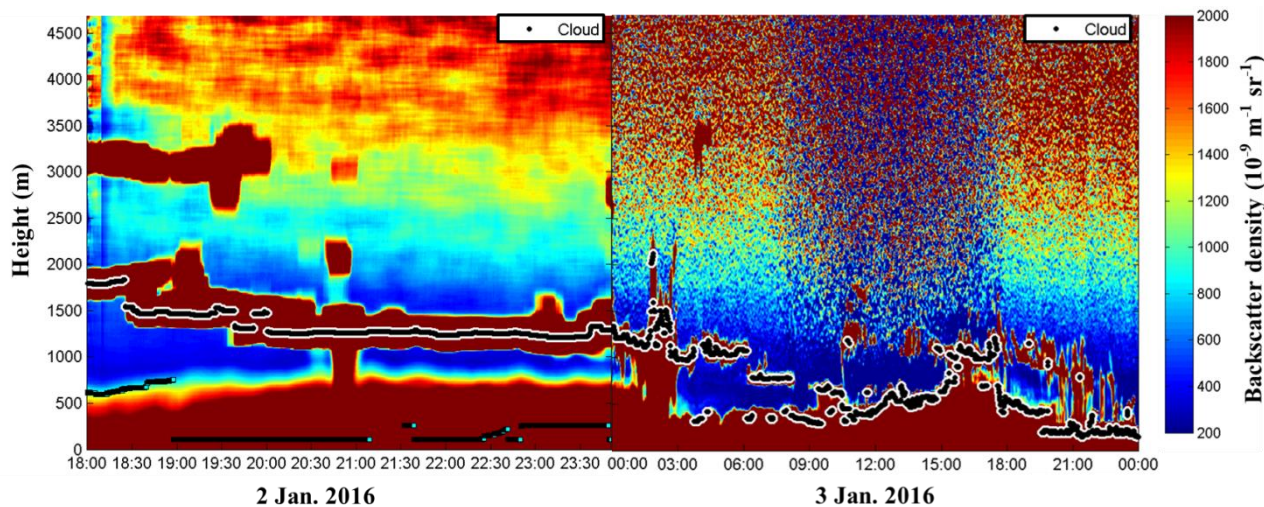
20



(a) January 02, 2016



(b) January 03, 2016



5 (c) Aerosol backscatter densities measured by ceilometer in Jan. 2 and Jan. 3, 2016.

**Figure S11.** Cloud cover from MODIS satellite remote sensing (<https://earthdata.nasa.gov/earth-observation-data/near-real-time/rapid-response>) and cloud heights measured by ceilometer (Model CL-31, Vaisala Corp.) during the winter pollution episode.

## **2. Weather Research and Forecasting (WRF) model setup and verification**

### **2.1 Description and configurations of WRF–Chem model**

The model used in this study is the chemistry version of the WRF model (WRF–Chem v3.7.1). The WRF model is a mesoscale non-hydrostatic meteorological model that includes several options for physical parameterizations of the planetary boundary layer (PBL), cloud processes and land surface (Skamarock et al., 2008). The chemistry version is a version of WRF coupled with an “online” chemistry model, in which meteorological and chemical components of the model are predicted simultaneously (Grell et al., 2005; Fast et al., 2006). Emission, chemical formation and removal, transport and deposition are considered when WRF–Chem predicts the chemical components. In the numerical modeling, a triple-nested grid with 27/9/3 km resolution domain and 39 layers in vertical is set (Figure S12). The chemistry only run in domain d03 (3 km resolution) and MOZART boundary condition is used for the chemistry run. The simulation period is conducted from 0000 UTC 18 October to 0000 UTC 28 November 2015 as the autumn time period and 0000 UTC 25 December 2015 to 0000 UTC 28 January 2016 as the winter time period. The National Center for Environmental Protection (NCEP)  $1^\circ \times 1^\circ$  FNL (Final operational global reanalysis) data are applied as the initial and boundary condition in WRF modeling. The physical and chemical parameterization configurations for WRF–Chem model can be found in Table S4. A region local anthropogenic emission inventory is used within the PRD region (Zheng et al., 2009), which is updated to the year of 2015. For other areas, the Multi-resolution Emission Inventory for China (MEIC, <http://meicmodel.org/>) is used in this study. MEGAN model version 2.1 is also used for providing the biogenic emissions (Guenther et al., 2006).

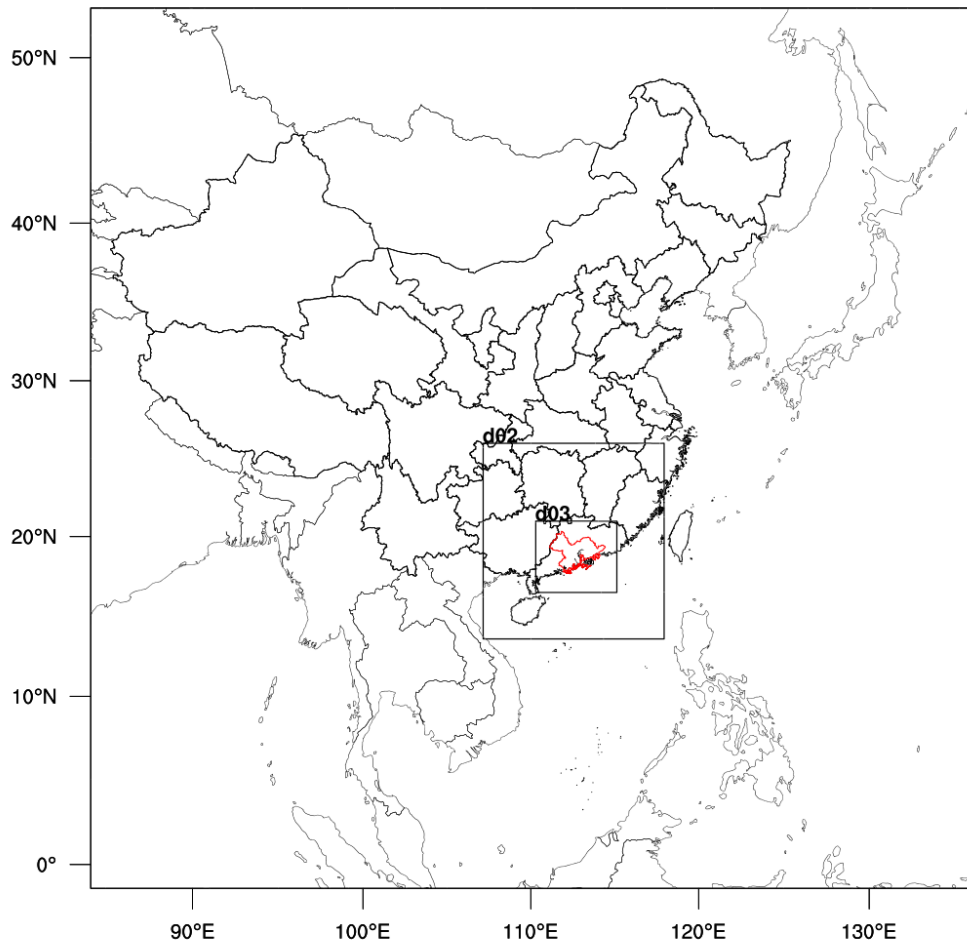


**Figure S12.** The simulation domain of WRF-Chem model

**Table S4.** Physical and chemical parameterization configurations for WRF-Chem model

Process	Option
Microphysics scheme	Morrison (2 moments)
Cumulus scheme	Kain-Fritsch
Longwave radiation scheme	RRTM
Shortwave radiation scheme	Dudhia
Boundary-layer scheme	YSU
Land-surface scheme	unified Noah
Urban Surface scheme	UCM
Gas-phase mechanism scheme	CBM-Z
Photolysis scheme	Fast-J
Aerosol scheme	MOSAIC

## 2.2 Model validation and performance

The performance statistics for meteorological elements such as pressure, air temperature, relative humidity and wind speed of three vertical layers on the Canton Tower and chemical pollutants such as PM<sub>2.5</sub>, NO<sub>x</sub>, O<sub>3</sub> and SO<sub>2</sub> are shown in Table S5 and Table S6. Here, the statistical measures such as Observation Mean, Simulation Mean, the Mean Bias (MB), the Normalized Mean Bias (NMB), the Normalized Mean Error (NME), the Mean Relative Bias (MRB), the Mean Relative Error (MRE), the Root Mean Squared Error (RMSE) and the correlation coefficient (CORR) are used for modeling validation.

10

**Table S5.** Comparison of Simulated Hourly Meteorological Elements with Observation Data

			Mean						
<b>Meteorologic al Elements (Unit)</b>	<b>Height</b>	<b>number<sup>a</sup></b>	<b>Obs.</b>	<b>Sim.</b>	<b>MB</b>	<b>NMB<sup>b</sup></b>	<b>NME<sup>b</sup></b>	<b>RMSE</b>	<b>CORR</b>
<b>Autumn</b>									
<b>PRES (hPa)</b>	GND	925	1015.4	1013.7	-1.7	-0.2	0.2	1.8	0.98
	121m	950	1002.0	1002.0	0.0	0.0	0.1	0.7	0.98
	454m	952	959.9	959.2	-0.7	-0.1	0.1	1.3	0.94
<b>TA (°C)</b>	GND	952	24.8	23.7	-1.2	-4.7	6.8	2.1	0.92
	121m	950	23.4	22.9	-0.6	-2.4	5.0	1.5	0.94
	454m	952	20.6	20.8	0.2	0.9	3.9	1.1	0.95
<b>RH (%)</b>	GND	952	62.5	65.6	3.1	5.0	12.4	9.8	0.82
	121m	950	64.9	67.1	2.2	3.4	11.2	9.1	0.85
	454m	952	72.4	73.0	0.6	0.9	9.6	8.8	0.86
<b>WS (m/s)</b>	GND	952	0.7	2.3	1.6	227.0	234.8	2.1	0.62
	121m	753	2.1	5.6	3.6	170.6	177.1	4.7	0.30
	454m	936	4.1	6.6	2.5	60.2	74.6	4.0	0.55
<b>Winter</b>									
<b>PRES (hPa)</b>	GND	758	1021.2	1019.5	-1.6	-0.2	0.2	1.8	0.99
	121m	770	1006.8	1007.8	1.1	0.1	0.1	1.3	0.99
	454m	776	962.9	964.9	2.0	0.2	0.2	2.4	0.97
<b>TA (°C)</b>	GND	765	14.8	12.7	-2.2	-14.6	16.2	2.9	0.91
	121m	525	14.7	13.5	-1.1	-7.7	10.5	1.8	0.94
	454m	648	10.7	11.4	0.8	7.4	41.2	5.1	0.84
<b>RH (%)</b>	GND	765	67.0	68.4	1.4	2.1	14.4	11.9	0.84
	121m	522	82.2	71.0	-11.2	-13.6	13.9	15.1	0.85
	454m	245	73.9	54.2	-19.7	-26.7	28.1	25.1	0.85
<b>WS (m/s)</b>	GND	765	0.9	2.4	1.5	175.7	179.1	1.9	0.71
	121m	526	2.0	6.4	4.4	215.5	220.6	5.7	0.23
	454m	751	4.8	8.2	3.3	68.9	76.3	4.6	0.66

<sup>a</sup> the number of observed data

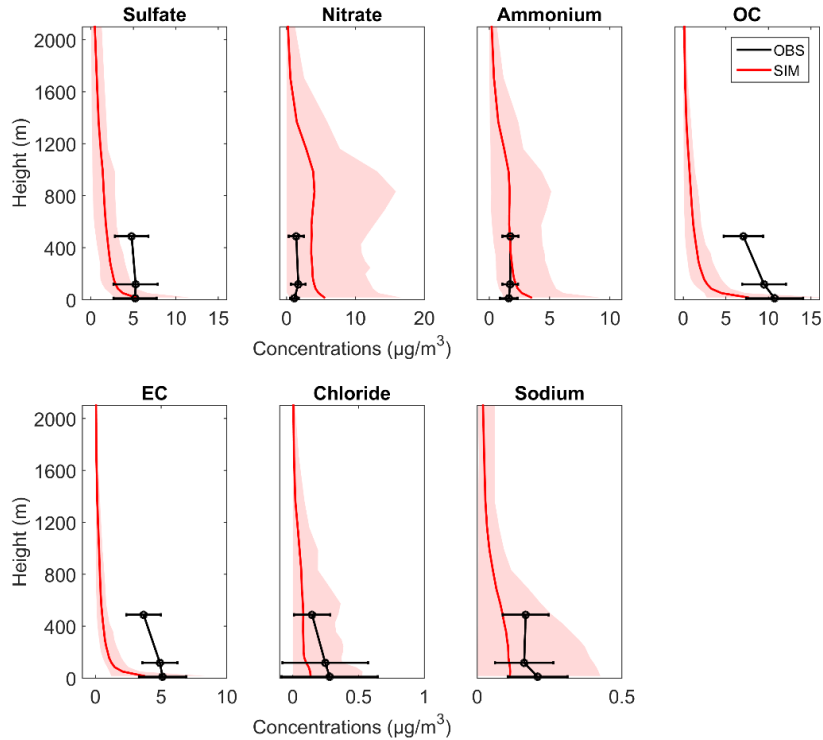
<sup>b</sup> the unit of NMB and NME is in %, other statistical variables are same as the meteorological element

**Table S6.** Comparison of Simulated Hourly Chemical Pollutants with Observation Data (unit:  $\mu\text{g}/\text{m}^3$ )

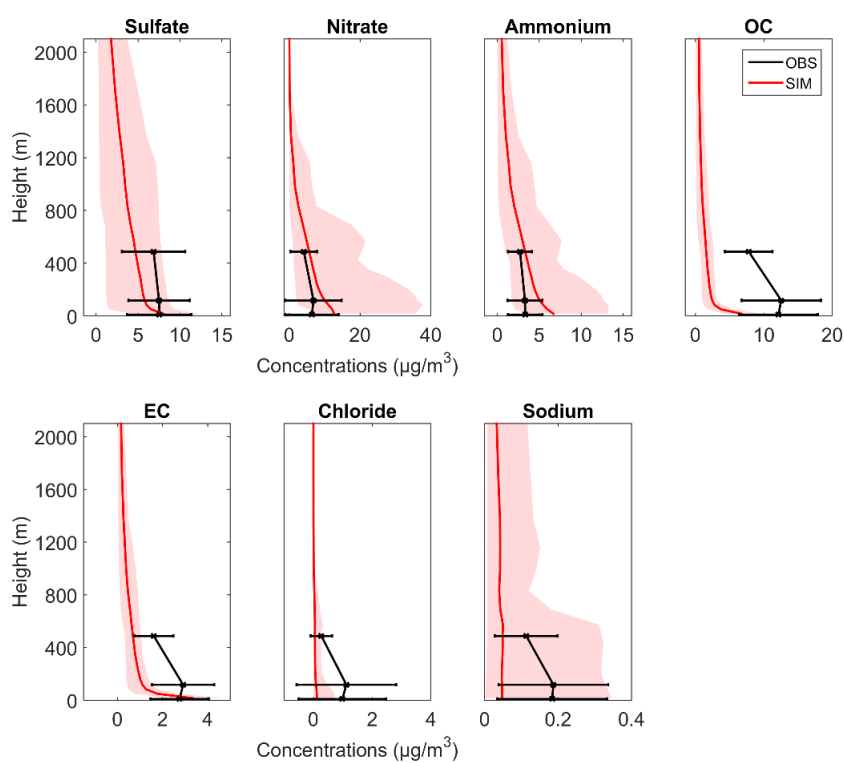
Meteorologic al Elements (Unit)	Height	number <sup>a</sup>	Mean		MB	NMB <sup>b</sup>	NME <sup>b</sup>	RMSE	CORR
			Obs.	Sim.					
<b>Autumn</b>									
PM <sub>2.5</sub>	GND	958	43.6	42.6	-1.0	-2.3	59.9	35.9	0.24
	168m	954	35.5	20.8	-14.7	-41.5	54.1	23.6	0.09
	488m	947	27.5	13.0	-14.5	-52.8	59.9	19.9	0.22
NO <sub>x</sub>	GND	949	101.7	90.7	-10.9	-10.7	62.0	93.4	0.41
	168m	922	75.4	28.0	-47.4	-62.9	68.9	69.3	0.13
	488m	950	27.1	7.7	-19.3	-71.5	79.7	28.9	0.24
O <sub>3</sub>	GND	939	36.1	39.6	3.5	9.6	58.5	31.1	0.72
	168m	947	58.3	72.0	13.8	23.6	62.9	46.6	0.64
	488m	947	103.8	95.7	-8.2	-7.9	37.8	51.9	0.55
SO <sub>2</sub>	GND	953	13.8	11.7	-2.1	-15.3	61.5	12.0	0.10
	168m	949	17.8	5.1	-12.7	-71.4	72.4	16.7	0.03
	488m	951	12.8	2.9	-9.9	-77.6	78.2	13.8	0.16
<b>Winter</b>									
PM <sub>2.5</sub>	GND	775	40.8	47.5	6.8	16.6	50.1	27.9	0.43
	168m	756	33.0	28.7	-4.3	-12.9	42.0	20.5	0.35
	488m	779	21.7	18.3	-3.4	-15.6	45.6	13.9	0.35
NO <sub>x</sub>	GND	755	115.4	167.1	51.7	44.8	83.4	147.7	0.45
	168m	785	75.7	29.4	-46.3	-61.1	66.6	68.9	0.33
	488m	705	25.6	5.7	-20.0	-77.9	85.5	29.5	0.28
O <sub>3</sub>	GND	761	19.8	19.6	-0.2	-1.0	77.3	22.2	0.65
	168m	786	26.6	61.3	34.7	130.1	137.5	43.3	0.49
	488m	784	63.4	88.5	25.0	39.5	44.0	33.7	0.38
SO <sub>2</sub>	GND	784	9.4	22.0	12.5	132.4	150.7	22.2	0.23
	168m	786	11.8	7.8	-4.1	-34.5	48.2	8.8	0.05
	488m	783	9.7	5.4	-4.3	-44.0	53.7	7.4	0.05

<sup>a</sup> the number of observed data

<sup>b</sup> the unit of NMB and NME is in %, other statistical variables are same as the meteorological variable



(a)



(b)

Figure S13. The vertical concentration profiles of sulfate, nitrate, ammonium, OC, EC, sodium and chloride in PM<sub>2.5</sub> during (a) autumn and (b) winter field study (The red solid lines are the average modeled concentrations and the shaded regions indicate the minimum and maximum values of the simulation; the average measurement data were in black with horizontal error bars).

## References:

- Grell, G. A., Peckham, S. E., Schmitz, R., McKeen, S. A., Frost, G., Skamarock, W. C., and Eder, B.: Fully coupled “online” chemistry within the WRF model, *Atmos. Environ.*, 39, 6957–6975, 2005.
- Fast, J. D., Gustafson Jr., Easter, W. I., Zaveri, R. C., Barnard, J. C., Chapman, E. G., Grell, G. A., and Packham, S. E.: Evolution of ozone, particulates and aerosol direct radiative forcing in the vicinity of Houston using a fully coupled meteorology-chemistry-aerosol model, *J. Geophys. Res.*, 111, D21305, doi:10.1029/2005JD006721, 2006.
- Skamarock, W.C., et al., 2008. A Description of the Advanced Research WRF Version 3. NCAR Technical Notes, NCAR/TN-4751STR.
- Zheng, J., Zhang, L., Che, W., Zheng, Z. and Yin, S.: A highly resolved temporal and spatial air pollutant emission inventory for the Pearl River Delta region , China and its uncertainty assessment, *Atmos. Environ.*, 43(32), 5112–5122, doi:10.1016/j.atmosenv.2009.04.060, 2009.
- Guenther, A., Karl, T., Harley, P., Wiedinmyer, C., Palmer, P. I., and Geron, C.: Estimates of global terrestrial isoprene emissions using MEGAN (Model of Emissions of Gases and Aerosols from Nature), *Atmos. Chem. Phys.*, 6, 3181–3210, doi:10.5194/acp-6-3181-2006, 2006.

25

30

### 3. Data used for analysis

**Table S7 Size-segregated PM components data used in the analysis**

Autumn	Size	F( $\mu\text{g}/\text{m}^3$ )	Cl( $\mu\text{g}/\text{m}^3$ )	NO2( $\mu\text{g}/\text{m}^3$ )	SO4( $\mu\text{g}/\text{m}^3$ )	NO3( $\mu\text{g}/\text{m}^3$ )	Na( $\mu\text{g}/\text{m}^3$ )	NH4( $\mu\text{g}/\text{m}^3$ )	K( $\mu\text{g}/\text{m}^3$ )	Mg( $\mu\text{g}/\text{m}^3$ )	Ca( $\mu\text{g}/\text{m}^3$ )	OC( $\mu\text{gC}/\text{m}^3$ )	EC( $\mu\text{gC}/\text{m}^3$ )
Ground	10~18	0.02	0.22	0.04	0.19	0.65	0.13	0.02	0.03	0.03	0.52	4.10	1.84
	2.5~10	0.05	0.66	0.00	0.87	3.16	0.60	0.11	0.07	0.10	0.94	3.62	0.70
	1.4~2.5	0.02	0.31	0.05	2.08	1.41	0.36	0.62	0.10	0.04	0.06	5.13	2.19
	1.0~1.4	0.04	0.39	0.05	5.73	0.72	0.20	1.87	0.26	0.02	0.23	8.44	3.97
	0.44~1.0	0.02	0.29	0.01	8.77	1.60	0.18	2.60	0.50	0.01	0.09	10.25	4.51
	0.25~0.44	0.01	0.09	0.03	2.57	0.32	0.09	0.85	0.21	0.00	0.05	9.35	4.27
	<0.25	0.01	0.03	0.00	0.19	0.05	0.00	0.08	0.01	0.00	0.03	3.26	1.90
118m	10~18	0.04	0.32	0.01	0.32	0.89	0.18	0.06	0.03	0.03	0.67	3.44	1.81
	2.5~10	0.07	0.89	0.02	0.91	3.86	0.67	0.23	0.08	0.11	0.97	3.50	1.22
	1.4~2.5	0.02	0.36	0.05	2.24	1.81	0.33	0.69	0.10	0.05	0.36	4.22	3.05
	1.0~1.4	0.02	0.31	0.10	5.63	1.59	0.17	2.09	0.19	0.02	0.03	6.90	4.03
	0.44~1.0	0.02	0.20	0.02	8.29	2.31	0.06	2.51	0.45	0.00	0.00	9.05	3.22
	0.25~0.44	0.02	0.08	0.04	3.35	0.67	0.10	1.23	0.27	0.00	0.00	9.24	4.31
	<0.25	0.00	0.02	0.00	0.14	0.03	0.01	0.07	0.12	0.00	0.01	2.74	1.92
488m	10~18	0.01	0.07	0.04	0.03	0.58	0.05	0.03	0.00	0.00	0.02	2.27	1.17
	2.5~10	0.03	0.56	0.00	0.77	3.26	0.58	0.29	0.05	0.08	0.52	1.99	0.61
	1.4~2.5	0.00	0.23	0.02	2.08	1.35	0.33	0.71	0.07	0.04	0.14	3.28	1.79
	1.0~1.4	0.02	0.06	0.01	5.72	1.05	0.14	1.99	0.15	0.00	0.03	5.62	3.06
	0.44~1.0	0.04	0.22	0.02	7.94	2.28	0.14	2.94	0.37	0.01	0.06	7.14	3.03
	0.25~0.44	0.02	0.01	0.06	2.39	0.32	0.06	0.88	0.15	0.00	0.06	6.06	2.94
	<0.25	0.00	0.00	0.00	0.03	0.03	0.00	0.02	0.00	0.00	0.00	1.97	1.38
Winter	Size	F( $\mu\text{g}/\text{m}^3$ )	Cl( $\mu\text{g}/\text{m}^3$ )	NO2( $\mu\text{g}/\text{m}^3$ )	SO4( $\mu\text{g}/\text{m}^3$ )	NO3( $\mu\text{g}/\text{m}^3$ )	Na( $\mu\text{g}/\text{m}^3$ )	NH4( $\mu\text{g}/\text{m}^3$ )	K( $\mu\text{g}/\text{m}^3$ )	Mg( $\mu\text{g}/\text{m}^3$ )	Ca( $\mu\text{g}/\text{m}^3$ )	OC( $\mu\text{gC}/\text{m}^3$ )	EC( $\mu\text{gC}/\text{m}^3$ )
	10~18	0.03	0.11	0.00	0.30	0.33	0.05	0.10	0.02	0.01	0.64	3.88	0.38
	2.5~10	0.09	0.41	0.02	1.17	2.19	0.14	0.27	0.06	0.05	1.20	2.94	0.73
	1.4~2.5	0.07	0.77	0.05	4.92	4.36	0.16	2.09	0.24	0.03	0.71	5.59	1.04
	1.0~1.4	0.04	1.15	0.03	8.94	6.93	0.18	4.57	0.44	0.00	0.21	9.52	1.99
	0.44~1.0	0.05	1.51	0.04	10.68	9.81	0.23	4.42	0.78	0.00	0.01	13.34	1.54
	0.25~0.44	0.05	0.32	0.07	3.51	2.76	0.11	1.80	0.38	0.00	0.06	10.54	1.78
	<0.25	0.01	0.01	0.03	0.44	0.15	0.01	0.18	0.05	0.00	0.03	2.83	1.75

	<b>10~18</b>	0.03	0.12	0.00	0.35	0.43	0.04	0.10	0.03	0.01	0.68	4.16	0.43
	<b>2.5~10</b>	0.09	0.39	0.02	1.01	2.00	0.13	0.28	0.06	0.04	1.09	2.83	0.96
	<b>1.4~2.5</b>	0.06	0.86	0.02	3.68	4.15	0.15	1.88	0.17	0.02	0.66	7.21	1.83
<b>118m</b>	<b>1.0~1.4</b>	0.06	1.54	0.04	9.54	7.86	0.21	5.26	0.47	0.00	0.22	10.43	2.69
	<b>0.44~1.0</b>	0.08	1.58	0.03	11.07	10.23	0.21	3.94	0.78	0.00	0.05	12.33	1.50
	<b>0.25~0.44</b>	0.03	0.45	0.02	4.00	3.65	0.16	2.24	0.43	0.00	0.12	11.02	1.50
	<b>&lt;0.25</b>	0.01	0.01	0.03	0.36	0.14	0.01	0.15	0.04	0.00	0.04	3.02	1.65
	<b>10~18</b>	0.01	0.05	0.00	0.23	0.48	0.03	0.13	0.02	0.00	0.20	2.00	0.15
	<b>2.5~10</b>	0.03	0.24	0.01	0.87	1.64	0.13	0.29	0.05	0.03	0.62	1.47	0.55
	<b>1.4~2.5</b>	0.02	0.23	0.01	3.41	2.48	0.08	1.40	0.09	0.01	0.43	3.18	0.88
<b>488m</b>	<b>1.0~1.4</b>	0.08	0.39	0.03	10.64	5.64	0.15	4.54	0.35	0.00	0.01	7.21	1.43
	<b>0.44~1.0</b>	0.06	0.39	0.00	9.97	6.57	0.14	3.60	0.50	0.00	0.02	8.58	0.77
	<b>0.25~0.44</b>	0.03	0.05	0.00	2.62	1.00	0.04	1.25	0.14	0.00	0.00	5.90	1.04
	<b>&lt;0.25</b>	0.01	0.01	0.02	0.34	0.09	0.02	0.15	0.03	0.00	0.00	2.04	0.93

**Table S8 Time variations of PM<sub>2.5</sub> data in autumn used for data analysis**

Date&Time	PM <sub>2.5</sub> (μg m <sup>-3</sup> )			
	Autumn	488 m	118	Ground
2015/10/20		30.2	41.7	49.9
2015/10/21		30.8	39.7	48.4
2015/10/22		24.5	29.5	34.7
2015/10/23		36.8	46.3	59.1
2015/10/24		28.4	35.4	48.9
2015/10/25		32.6	39.3	45.7
2015/10/26		26.1	35.7	41.5
2015/10/27		40.6	43.5	53.9
2015/10/28		41.9	50.9	58.5
2015/10/29		27.4	35.3	40.6
2015/10/30		33.8	34.5	42.0
2015/10/31		18.3	19.7	20.2
2015/11/1		9.8	12.3	13.6
2015/11/2		21.5	28.0	34.6
2015/11/3		30.4	40.0	53.2
2015/11/4		35.0	47.3	62.0
2015/11/5		33.2	47.5	52.4
2015/11/6		22.2	35.3	43.3

2015/11/7	23.0	36.1	40.3
2015/11/8	23.0	30.9	39.2
2015/11/9	18.9	21.2	23.5
2015/11/10	26.1	28.8	40.0
2015/11/11	42.1	48.9	62.6
2015/11/12	31.8	40.0	47.6
2015/11/13	7.9	13.5	12.5
2015/11/14	16.8	26.4	36.8
2015/11/15	21.0	31.4	39.5
2015/11/16	10.8	24.5	29.5
2015/11/17	11.1	26.3	28.4
2015/11/18	37.7	49.8	76.0
2015/11/19	34.9	51.0	63.9
2015/11/20	44.4	54.2	64.6
2015/11/21	37.2	42.5	49.8
2015/11/22	23.7	29.0	34.2
2015/11/23	18.5	24.1	32.9
2015/11/24	28.4	35.4	48.9
2015/11/25	12.9	15.7	16.4
2015/11/26	14.3	18.3	23.3

**Table S9 Time variations of PM<sub>2.5</sub> data in winter used for data analysis**

Date&Time Winter	PM2.5 ( $\mu\text{g m}^{-3}$ )		
	488 m	118	Ground
2015/12/31	41.4	47.6	61.3
2016/1/1	40.0	57.8	77.9
2016/1/2	47.2	83.4	104.8
2016/1/3	42.1	80.3	87.2
2016/1/4	25.9	53.0	54.4
2016/1/5	7.8	19.5	18.8
2016/1/6	14.4	19.8	36.0
2016/1/7	25.3	30.0	42.6
2016/1/8	26.0	31.9	42.9
2016/1/9	37.3	52.1	65.8
2016/1/10	21.3	29.6	30.4
2016/1/11	8.9	14.3	20.6
2016/1/12	19.2	20.4	31.7
2016/1/13	23.1	26.5	37.3
2016/1/14	25.1	38.5	48.5
2016/1/15	8.7	17.3	18.0
2016/1/16	9.1	32.1	45.7
2016/1/17	11.3	16.8	20.6
2016/1/18	21.3	27.6	35.2
2016/1/19	31.7	44.0	58.0
2016/1/20	16.3	31.1	33.9
2016/1/21	7.2	17.8	23.1
2016/1/22	7.8	10.7	10.2
2016/1/23	21.3	26.0	37.9
2016/1/24	20.6	24.3	25.0
2016/1/25	17.0	21.9	24.5